SUSY Parameter Analysis at TeV and Planck Scales

B. C. Allanach[a], G. A. Blair[b c], A. Freitas[d], S. Kraml[e f], H.-U. Martyn[g], G. Polesello[f], W. Porod[h], and P. M. Zerwas[b]

[a]LAPTH, Annecy-le-Vieux, France

[b]Deutsches Elektronen-Synchrotron DESY, D-22603 Hamburg, Germany

[c]Royal Holloway University of London, Egham, Surrey. TW20 0EX, UK

[d]Fermi National Accelerator Laboratory, P. O. Box 500, Batavia IL 60510, USA

[e]Inst. f. Hochenergiephysik, Österr. Akademie d. Wissenschaften, A-1050 Vienna, Austria

[f]CERN, Department of Physics, CH-1211 Geneva 23, Switzerland

[g]I. Physik. Institut, RWTH Aachen, D-52074 Aachen, Germany

[h]IFIC - Instituto de Física Corpuscular, E-46071 Valencia, Spain

Coherent analyses at future LHC and LC experiments can be used to explore the breaking mechanism of supersymmetry and to reconstruct the fundamental theory at high energies, in particular at the grand unification scale. This will be exemplified for minimal supergravity.

1. Physics Base

The roots of standard particle physics are expected to go as deep as the Planck length of 10^{-33} cm where gravity is intimately linked to the particle system. A stable bridge between the electroweak energy scale of 100 GeV and the vastly different Planck scale of $\Lambda_{\rm PL} \sim 10^{19}$ GeV, and the (nearby) grand unification scale $\Lambda_{\rm GUT} \sim 10^{16}$ GeV, is provided by supersymmetry. Methods must therefore be developed which allow to study the supersymmetry breaking mechanism and the physics scenario near the GUT/PL scale [1].

The reconstruction of physical structures at energies more than fourteen orders above accelerator energies is a demanding task. LHC [2] and a future e^+e^- linear collider (LC) [3] are a perfect tandem for solving such a problem: While the colored supersymmetric particles, gluinos and squarks, can be generated with large rates for masses up to 2 to 3 TeV at the LHC, the strength of e^+e^- linear colliders is the comprehensive coverage of the non-colored particles, charginos/neutralinos and sleptons. If the analyses are performed coherently, the accuracies in measurements of cascade decays at LHC and in threshold production as well as decays of supersymmetric particles at LC complement each other mutually. A comprehensive and precise picture is needed in order to carry out the evolution of the supersymmetric parameters to high scales, which is driven by perturbative loop effects involving the entire supersymmetric particle spectrum.

Minimal supergravity [mSUGRA] provides us with a scenario within which these general ideas can be quantified. Supersymmetry is broken in mSUGRA in a hidden sector and the breaking is transmitted to our eigenworld by gravity [4]. The mechanism suggests, yet does not enforce [see *e.g.* Ref.[5]], the universality of the soft SUSY breaking parameters – gaugino and scalar masses, trilinear couplings – at a scale that is generally identified with the unification scale. Alternative scenarios have been formulated for left–right symmetric extensions, superstring effective theories,

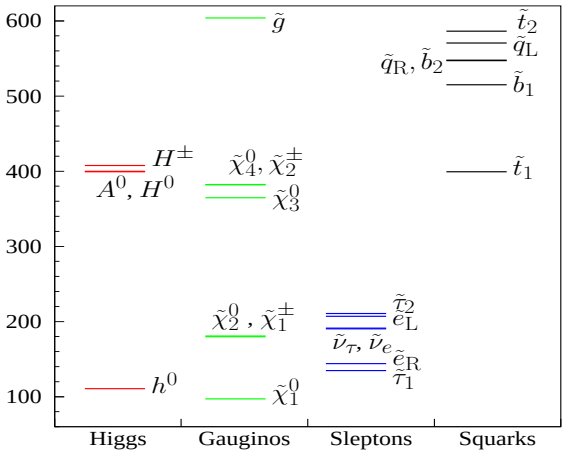

Figure 1. *Spectrum of Higgs, gaugino/higgsino and sparticle masses in the mSUGRA scenario SPS1a [masses in* GeV*].*

and for other SUSY breaking mechanisms.

2. Minimal Supergravity

The mSUGRA Snowmass reference point SPS1a is characterised by the following values [6]

$$\begin{array}{ll} M_{1/2} = 250 \text{ GeV} & M_0 = 100 \text{ GeV} \\ A_0 = -100 \text{ GeV} & \text{sign}(\mu) = + \\ \tan\beta = 10 & \end{array} \qquad (1)$$

for the universal gaugino mass $M_{1/2}$, the scalar mass M_0, the trilinear coupling A_0, the sign of the higgsino parameter μ, and $\tan\beta$, the ratio of the vacuum-expectation values of the two Higgs fields. As the modulus of the higgsino parameter is fixed at the electroweak scale by requiring radiative electroweak symmetry breaking, μ is finally given by $\mu = 357.4$ GeV. The form of the supersymmetric mass spectrum of SPS1a is shown in Fig. 1. In this scenario the squarks and gluinos can be studied very well at the LHC while the non-colored gauginos and sleptons can be analyzed partly at LHC and in comprehensive form at an e^+e^- linear collider operating at a total energy up to 1 TeV with high integrated luminosity close to 1 ab^{-1}.

At LHC the masses can best be obtained by analyzing edge effects in the cascade decay spectra. The basic starting point is the identification of a sequence of two-body decays: $\tilde{q}_L \to \tilde{\chi}_2^0 q \to \tilde{\ell}_R \ell q \to \tilde{\chi}_1^0 \ell\ell q$. One can then measure the kinematic edges of the invariant mass distributions among the two leptons and the jet resulting from the above chain, and thus an approximately model-independent determination of the masses of the involved sparticles is obtained [7,8]. The four sparticle masses [$\tilde{q}_L$, $\tilde{\chi}_2^0$, $\tilde{\ell}_R$ and $\tilde{\chi}_1^0$] are used subsequently as input for additional decay chains like $\tilde{g} \to \tilde{b}_1 b \to \tilde{\chi}_2^0 bb$, and the shorter chains $\tilde{q}_R \to q\tilde{\chi}_1^0$ and $\tilde{\chi}_4^0 \to \tilde{\ell}\ell$, which all require the knowledge of the sparticle masses downstream of the cascades.

	Mass	"LHC"	"LC"	"LHC+LC"
$\tilde{\chi}_1^\pm$	179.7		0.55	0.55
$\tilde{\chi}_2^\pm$	382.3	–	3.0	3.0
$\tilde{\chi}_1^0$	97.2	4.8	0.05	0.05
$\tilde{\chi}_2^0$	180.7	4.7	1.2	0.08
$\tilde{\chi}_3^0$	364.7		3-5	3-5
$\tilde{\chi}_4^0$	381.9	5.1	3-5	2.23
$\tilde{e}_R$	143.9	4.8	0.05	0.05
$\tilde{e}_L$	207.1	5.0	0.2	0.2
$\tilde{q}_R$	547.6	7-12	–	5-11
$\tilde{q}_L$	570.6	8.7	–	4.9
$\tilde{t}_1$	399.5		2.0	2.0
$\tilde{g}$	604.0	8.0	–	6.5
h^0	110.8	0.25	0.05	0.05
H^0	399.8		1.5	1.5
A^0	399.4		1.5	1.5
$H^\pm$	407.7	–	1.5	1.5

Table 1
Accuracies for representative mass measurements at "LHC" and "LC", cf. Ref. [12], and in coherent "LHC+LC" analyses for the reference point SPS1a [masses in GeV*].*

At LC very precise mass values can be extracted from decay spectra and threshold scans [9,10]. The excitation curves for chargino production in S-waves [11] rise steeply with the velocity of the particles near the thresholds and thus are very sensitive to their mass values; the same is true for mixed-chiral selectron pairs in

	Parameter, ideal	"LHC+LC" errors
M_1	101.66	0.08
M_2	191.76	0.25
M_3	584.9	3.9
μ	357.4	1.3
$M^2_{L_1}$	$3.8191 \cdot 10^4$	82.
$M^2_{E_1}$	$1.8441 \cdot 10^4$	15.
$M^2_{Q_1}$	$29.67 \cdot 10^4$	$0.32 \cdot 10^4$
$M^2_{U_1}$	$27.67 \cdot 10^4$	$0.86 \cdot 10^4$
$M^2_{D_1}$	$27.45 \cdot 10^4$	$0.80 \cdot 10^4$
$M^2_{H_2}$	$-12.78 \cdot 10^4$	$0.11 \cdot 10^4$
A_t	$-497.$	9.
$\tan\beta$	10.0	0.4

Table 2
The extracted SUSY Lagrange mass and Higgs parameters at the electroweak scale in the reference point SPS1a [mass unit GeV*].*

$e^+e^- \to \tilde{e}^+_R\tilde{e}^-_L$ and for diagonal pairs in $e^-e^- \to \tilde{e}^-_R\tilde{e}^-_R$, $\tilde{e}^-_L\tilde{e}^-_L$ collisions, see Ref.[10] which includes also the effects of radiative corrections. Other scalar sfermions, as well as neutralinos, are produced generally in P-waves, with a less steep threshold behaviour proportional to the third power of the velocity. Additional information, in particular on the lightest neutralino $\tilde{\chi}^0_1$, can be obtained from the very sharp edges of 2-body decay spectra, such as $\tilde{e}^-_R \to e^-\tilde{\chi}^0_1$.

Typical mass parameters and the related measurement errors are presented in Table 1: "LHC" from LHC analyses and "LC" from LC analyses. The third column "LHC+LC" presents the corresponding errors if the experimental analyses are performed coherently, i.e. the light particle spectrum, studied at LC with very high precision, is used as input set for the LHC analysis.

Mixing parameters must be extracted from measurements of cross sections and polarization asymmetries, in particular from the production of chargino pairs and neutralino pairs [11], both in diagonal or mixed form: $e^+e^- \to \tilde{\chi}^+_i\tilde{\chi}^-_j$ [i,j = 1,2] and $\tilde{\chi}^0_i\tilde{\chi}^0_j$ [i,j = 1,...,4]. The production cross sections for charginos are binomials of $\cos 2\phi_{L,R}$, the mixing angles rotating current to mass eigenstates. Using polarized electron and positron beams, the mixings can be determined in a model-independent way.

The fundamental SUSY parameters can be derived to lowest order in analytic form:

$$\begin{aligned}
|\mu| &= M_W[\Sigma + \Delta[\cos 2\phi_R + \cos 2\phi_L]]^{1/2} \\
M_2 &= M_W[\Sigma - \Delta(\cos 2\phi_R + \cos 2\phi_L)]^{1/2} \\
|M_1| &= \left[\textstyle\sum_i m^2_{\tilde{\chi}^0_i} - M_2^2 - \mu^2 - 2M_Z^2\right]^{1/2} \\
|M_3| &= m_{\tilde{g}} \\
\tan\beta &= \left[\frac{1 + \Delta(\cos 2\phi_R - \cos 2\phi_L)}{1 - \Delta(\cos 2\phi_R - \cos 2\phi_L)}\right]^{1/2} \qquad (2)
\end{aligned}$$

where $\Delta = (m^2_{\tilde{\chi}^\pm_2} - m^2_{\tilde{\chi}^\pm_1})/(4M^2_W)$ and $\Sigma = (m^2_{\tilde{\chi}^\pm_2} + m^2_{\tilde{\chi}^\pm_1})/(2M^2_W) - 1$. The signs of μ, $M_{1,3}$ with respect to M_2 follow from similar relations and from cross sections for $\tilde{\chi}$ production and $\tilde{g}$ processes. In practice one-loop corrections to the mass relations have been used to improve on the accuracy.

The mass parameters of the sfermions are directly related to the physical masses if mixing effects are negligible:

$$m^2_{\tilde{f}_{L,R}} = M^2_{L,R} + m^2_f + D_{L,R} \qquad (3)$$

with $D_L = (T_3 - e_f \sin^2\theta_W)\cos 2\beta\, m^2_Z$ and $D_R = e_f \sin^2\theta_W \cos 2\beta\, m^2_Z$ denoting the D-terms. The non-trivial mixing angles in the sfermion sector of the third generation follow from the sfermion production cross sections for longitudinally polarized e^+/e^- beams, which are bilinear in $\cos/\sin 2\theta_{\tilde{f}}$. The mixing angles and the two physical sfermion masses are related to the tri-linear couplings A_f, the higgsino mass parameter μ and $\tan\beta(\cot\beta)$ for down(up) type sfermions by:

$$A_f - \mu\tan\beta(\cot\beta) = \frac{m^2_{\tilde{f}_1} - m^2_{\tilde{f}_2}}{2m_f}\sin 2\theta_{\tilde{f}} \qquad (4)$$

A_f may be determined in the $\tilde{f}$ sector if μ has been measured in the chargino sector.

Accuracies expected for the SUSY Lagrange parameters at the electroweak scale for the reference point SPS1a are shown in Table 2. They have been calculated by means of SPheno2.2.0 [13]. Theoretical errors, exemplified in Table 3,

	$\tilde{q}_R - \tilde{\chi}_1^0$	$\tilde{l}_L - \tilde{\chi}_1^0$	$m[\tilde{g} - [\tilde{b}_1]$
SPheno 2.2.0	450.3	110.0	88.9
Δ_{exp}^{LHC}	10.9	1.6	1.8
Δ_{th}	8.1	0.23	6.8

Table 3
A sample of observable mass differences at LHC for SPS1a and their experimental (Δ_{exp}^{LHC}) and present theoretical (Δ_{th}) uncertainties due to variations of the SUSY scale. [All quantities in GeV]. See also Ref. [14].

have been estimated by varying the characteristic SUSY scale between 100 GeV and 1 TeV. Note that these theoretical errors do match the experimental LHC errors but they must be reduced by an order of magnitude to match the expected accuracies at LC.

3. Reconstruction of the Fundamental SUSY Theory

The fundamental mSUGRA parameters [1] at the GUT scale are related to the low-energy parameters at the electroweak scale by supersymmetric renormalization group transformations (RG) [15,16] which to leading order generate the evolution for:

gauge couplings : $\alpha_i = Z_i\, \alpha_U$ (5)

gaugino masses : $M_i = Z_i\, M_{1/2}$ (6)

scalar masses :

$$M_j^2 = M_0^2 + c_j M_{1/2}^2 + \sum_{\beta=1}^{2} c'_{j\beta} \Delta M_\beta^2 \quad (7)$$

trilinear couplings : $A_k = d_k A_0 + d'_k M_{1/2}$ (8)

The index i runs over the gauge groups $i = SU(3), SU(2), U(1)$. To leading order, the gauge couplings, and the gaugino and scalar mass parameters of soft–supersymmetry breaking depend on the Z transporters

$$Z_i^{-1} = 1 + b_i \frac{\alpha_U}{4\pi} \log\left(\frac{M_U}{M_Z}\right)^2 \quad (9)$$

with $b[SU_3, SU_2, U_1] = -3,\, 1,\, 33/5$; the scalar mass parameters depend also on the Yukawa couplings h_t, h_b, h_τ of the top quark, bottom quark and τ lepton. The coefficients c_j for the slepton and squark doublets/singlets, and for the two Higgs doublets, are linear combinations of the evolution coefficients Z; the coefficients $c'_{j\beta}$ are of order unity. The shifts ΔM_β^2, depending implicitly on all the other parameters, are nearly zero for the first two families of sfermions but they can be rather large for the third family and for the Higgs mass parameters. The coefficients d_k of the trilinear couplings A_k $[k = t, b, \tau]$ depend on the corresponding Yukawa couplings and they are approximately unity for the first two generations while being $O(10^{-1})$ and smaller if the Yukawa couplings are large; the coefficients d'_k, depending on gauge and Yukawa couplings, are of order unity. Beyond the approximate solutions, the evolution equations have been solved numerically in the present analysis to two–loop order [16] and threshold effects have been incorporated at the low scale [17]. The 2-loop effects as given in Ref. [18] have been included for the neutral Higgs bosons and the μ parameter.

3.1. Gauge Coupling Unification

Measurements of the gauge couplings at the electroweak scale support very strongly the unification of the couplings at a scale $M_U \simeq 2 \times 10^{16}$ GeV [19]. The precision, at the per–cent level, is surprisingly high after extrapolations over fourteen orders of magnitude in the energy from the electroweak scale to the grand unification scale M_U. Conversely, the electroweak mixing angle has been predicted in this approach at the per–mille level. The evolution of the gauge couplings from low energy to the GUT scale M_U has been carried out at two–loop accuracy in the $\overline{DR}$ scheme. The couplings are evolved to M_U using 2-loop RGEs [16]. The gauge couplings do not meet exactly, cf. Fig. 2 and Tab. 4. The differences are to be attributed to high-threshold effects at the unification scale M_U and the quantitative evolution implies important constraints on the particle content at M_U [20].

3.2. Gaugino and Scalar Mass Parameters

In the bottom-up approach the fundamental supersymmetric theory is reconstructed at the high scale from the available *corpus* of experimental data without any theoretical prejudice. This approach exploits the experimental information

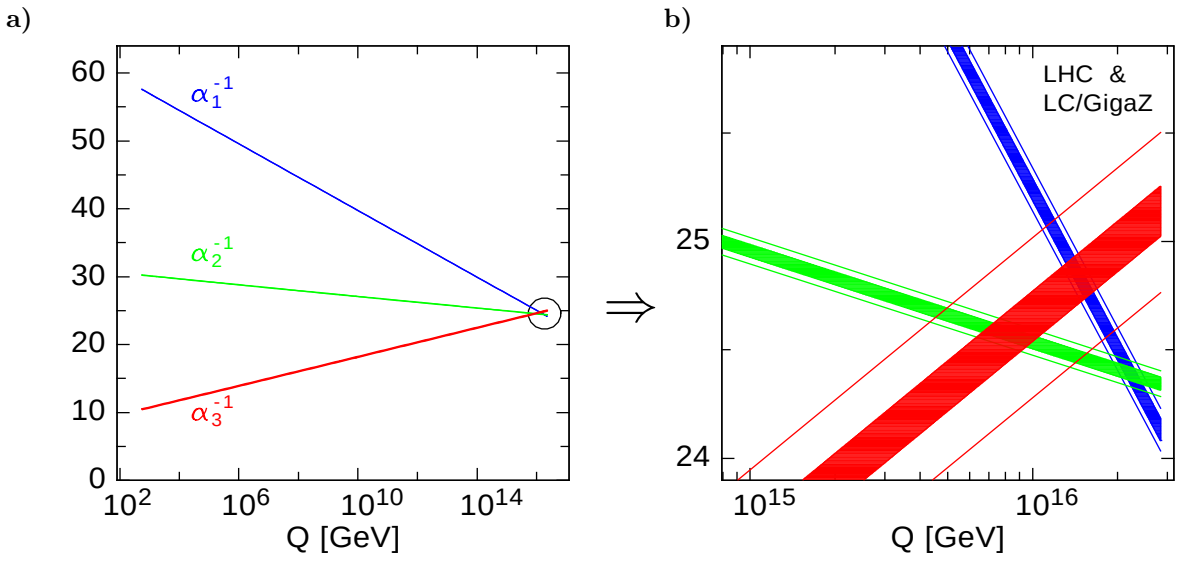

Figure 2. *(a) Running of the inverse gauge couplings from low to high energies. (b) Expansion of the area around the unification point M_U defined by the meeting point of α_1 with α_2. The wide error bands are based on present data, and the spectrum of supersymmetric particles from LHC measurements within mSUGRA. The narrow bands demonstrate the improvement expected by future GigaZ analyses [21] and the measurement of the complete spectrum at "LHC+LC".*

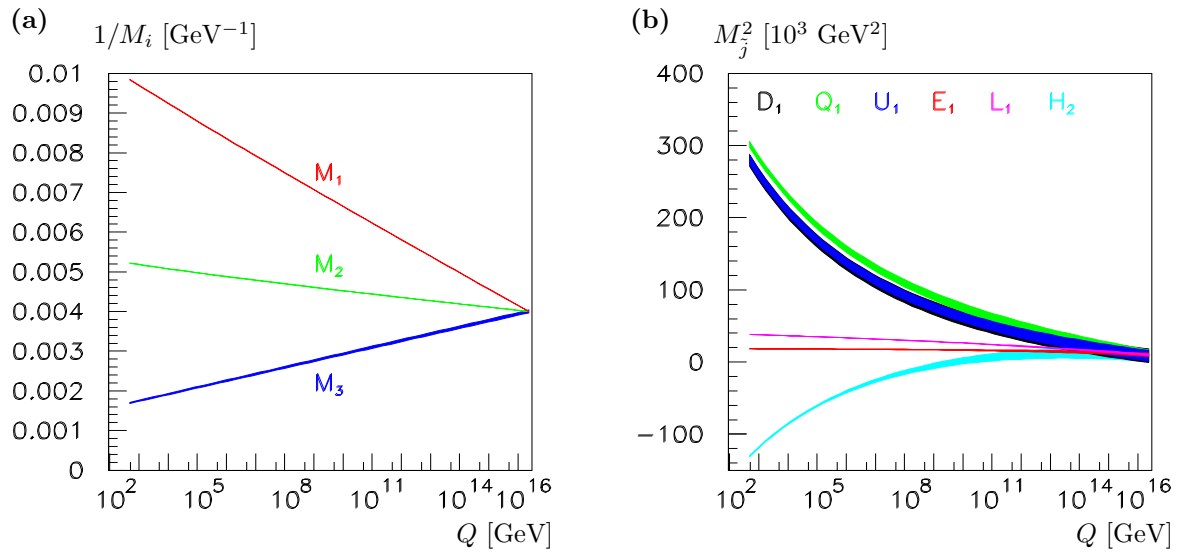

Figure 3. *Evolution, from low to high scales, (a) of the gaugino mass parameters for "LHC+LC" analyses; (b) of the first/second generation sfermion mass parameters and the Higgs mass parameter $M^2_{H_2}$.*

	Present/"LHC"	GigaZ/"LHC+LC"
M_U	$(2.36 \pm 0.06) \cdot 10^{16}$ GeV	$(2.360 \pm 0.016) \cdot 10^{16}$ GeV
α_U^{-1}	24.19 ± 0.10	24.19 ± 0.05
$\alpha_3^{-1} - \alpha_U^{-1}$	0.97 ± 0.45	0.95 ± 0.12

Table 4
Expected errors on M_U and α_U for the mSUGRA reference point SPS1a, derived for the present level of experimental accuracy and compared with expectations from GigaZ [21]. Also shown is the difference between α_3^{-1} and α_U^{-1} at the unification point M_U.

to the maximum extent possible and reflects an undistorted picture of our understanding of the basic theory. Such a program can only be carried out in coherent "LHC+LC" analyses while the separate information from either machine proves insufficient. The results for the evolution of the mass parameters from the electroweak scale to the GUT scale M_U are shown in Fig. 3.

On the left of Fig. 3 the evolution is presented for the gaugino parameters M_i^{-1}. It clearly is under excellent control for the model-independent reconstruction of the parameters and the test of universality in the $SU(3) \times SU(2) \times U(1)$ group space. In the same way the evolution of the scalar mass parameters can be studied, presented in Figs. 3b for the first/second generation. While the slepton parameters can be determined very accurately, the accuracy deteriorates for the squark parameters and the Higgs parameter $M_{H_2}^2$.

4. Summary

In supersymmetric theories stable extrapolations can be performed from the electroweak scale to the grand unification scale, close to the Planck scale. This feature has been demonstrated compellingly in the evolution of the three gauge couplings and of the soft supersymmetry breaking parameters, which approach universal values at the GUT scale in minimal supergravity. The coherent "LHC+LC" analyses in which the measurements of SUSY particle properties at LHC and LC mutually improve each other, result in a comprehensive and detailed picture of the supersymmetric particle system. In particular, the gaugino sector and the non-colored scalar sector are under excellent control.

	Parameter, ideal	Experimental error
M_U	$2.36 \cdot 10^{16}$	$2.2 \cdot 10^{14}$
α_U^{-1}	24.19	0.05
$M_{\frac{1}{2}}$	250.	0.2
M_0	100.	0.2
A_0	-100.	14
μ	357.4	0.4
$\tan\beta$	10.	0.4

Table 5
Comparison of the ideal parameters with the experimental expectations in the combined "LHC+LC" analyses for the particular mSUGRA reference point adopted in this report [units in GeV*].*

This point can be highlighted by performing a global mSUGRA fit of the universal parameters, c.f. Tab. 5. Accuracies at the level of per-cent to per-mille can be reached, allowing us to reconstruct the structure of nature at scales where gravity is linked with particle physics.

Though minimal supergravity has been chosen as a specific example, the method can equally well be applied in other scenarios, such as left-right symmetric theories and superstring theories. The analyses offer the exciting opportunity to determine intermediate scales in left-right symmetric theories and to measure effective string-theory parameters near the Planck scale.

REFERENCES

1. G. A. Blair, W. Porod and P. M. Zerwas, Phys. Rev. **D63** (2001) 017703 and Eur.

Phys. J. **C27** (2003) 263; P. M. Zerwas *et al.*, Proceedings, Int. HEP Conf., Amsterdam 2002, hep-ph/0211076; B. C. Allanach, G. A. Blair, S. Kraml, H. U. Martyn, G. Polesello, W. Porod and P. M. Zerwas, in "LHC/LC Physics Document", hep-ph/0403133.

2. I. Hinchliffe et al., Phys. Rev. **D 55**, 5520 (1997); Atlas Collaboration, Technical Design Report 1999, Vol. II, CERN/LHC/99-15, ATLAS TDR 15.
3. TESLA Technical Design Report (Part 3), R. D. Heuer, D. J. Miller, F. Richard and P. M. Zerwas (*eds.*), DESY 010-11, hep-ph/0106315; American LC Working Group, T. Abe *et al.*, SLAC-R-570 (2001), hep-ex/0106055-58; ACFA LC Working Group, K. Abe *et al.*, KEK-REPORT-2001-11, hep-ex/0109166.
4. A. H. Chamseddine, R. Arnowitt and P. Nath, Phys. Rev. Lett. **49** (1982) 970; H. P. Nilles, Phys. Rept. **110** (1984) 1.
5. K. Tobe and J. D. Wells, Phys. Lett. **B588** (2004) 99.
6. B. C. Allanach *et al.*, Eur. Phys. J. **C25** (2002) 113.
7. H. Bachacou, I. Hinchliffe and F. E. Paige Phys.Rev. **D62** (2000) 015009.
8. B. C. Allanach, C. G. Lester, M. A. Parker and B. R. Webber, JHEP 0009 (2000) 004.
9. H.-U. Martyn and G. A. Blair, hep-ph/9910416.
10. A. Freitas, D. J. Miller and P. M. Zerwas, Eur. Phys. J. **C21** (2001) 361; A. Freitas, A. von Manteuffel and P. M. Zerwas, Eur. Phys. J. **C34** (2004) 487.
11. S.Y. Choi, A. Djouadi, M. Guchait, J. Kalinowski, H.S. Song and P.M. Zerwas, Eur. Phys. J. **C14** (2000) 535; S.Y. Choi, J. Kalinowski, G. Moortgat-Pick and P.M. Zerwas, Eur. Phys. J. **C22** (2001) 563 and Eur. Phys. J. **C23** (2002) 769.
12. M. Chiorboli et al., in "LHC/LC Physics Document"; H.-U. Martyn et al., *ibid.*
13. W. Porod, Comput. Phys. Commun. **153** (2003) 275.
14. B. C. Allanach, S. Kraml and W. Porod, JHEP **0303** (2003) 016; see also `http://cern.ch/kraml/comparison/`
15. K. Inoue, A. Kakuto, H. Komatsu, and S. Takeshita, Prog. Theor. Phys. **68**, 927 (1982); Erratum, *ibid.* **70**, 330 (1983).
16. S. Martin and M. Vaughn, Phys. Rev. **D50**, 2282 (1994); Y. Yamada, Phys. Rev. **D50**, 3537 (1994); I. Jack, D.R.T. Jones, Phys. Lett. **B333** (1994) 372.
17. J. Bagger, K. Matchev, D. Pierce, and R. Zhang, Nucl. Phys. **B491** (1997) 3.
18. G. Degrassi, P. Slavich and F. Zwirner, Nucl. Phys. **B611** (2001) 403; A. Brignole, G. Degrassi, P. Slavich and F. Zwirner, Nucl. Phys. **B631** (2002) 195; Nucl. Phys. **B643** (2002) 79; A. Dedes and P. Slavich, Nucl. Phys. **B657** (2003) 333; A. Dedes, G. Degrassi and P. Slavich, hep-ph/0305127.
19. S. Dimopoulos, S. Raby and F. Wilczek, Phys. Rev. **D24** (1981) 1681; L. E. Ibanez, G. G. Ross, Phys. Lett. **B105** (1981) 439; U. Amaldi, W. de Boer and H. Fürstenau, Phys. Lett. **B260** (191) 447; P. Langacker and M. Luo, Phys. Rev. **D44** (1991) 817; J. Ellis, S. Kelley, D. V. Nanopoulos, Phys. Lett. **B260** (1991) 161.
20. G.G. Ross and R.G. Roberts, Nucl. Phys. **B377** (1992) 571.
21. K. Mönig, in "Physics and Experiments with Future Linear e^+e^- Colliders", hep-ex/0101005; J. Erler, S. Heinemeyer, W. Hollik, G. Weiglein and P.M. Zerwas, Phys. Lett. **B486** (2000) 125.